

# K2 MICROLensing: FREE-FLOATING PLANETS AND MICROLENS PLANET MASSES

ANDREW GOULD, KEITH HORNE, RACHEL STREET  
OSU, St. Andrews, LCOGT

**Abstract:** K2 can function as a unique and powerful microlensing parallax satellite. By observing 5.34 deg<sup>2</sup> of microlensing fields already monitored from the ground (but from 1 AU away) it can “triangulate” microlensing events and so measure the mass and distance of the lenses. It is particularly well-adapted to characterizing the recently detected population of free-floating planets. There is no way to detect this population other than microlensing and no foreseeable way to measure its mass function other than K2.

**Key words:** planets – gravitational microlensing

## 1. INTRODUCTION

While the idea of microlensing satellite parallaxes is 48 years old (Refsdal, 1966), a K2 microlens survey would be radically different from – and better than – any parallax survey conceived of prior to this mission opportunity. In particular, it has the unique capability of resolving the nature of the recently discovered “free-floating” planets.

Microlensing satellite parallaxes require simultaneous observation of the *same* microlensing events from the ground and a satellite located roughly 1 AU from Earth. In all previous incarnations, the idea was to first find the event from the ground, then notify the satellite to begin observing it. This generally would compromise targets that happened to peak earlier from the satellite than Earth, and it would eliminate the possibility of getting parallaxes for short events, such as the  $\sim 1$ -day free-floating planets (FFPs).

## 2. WHY MICROLensing PARALLAXES ARE CRUCIAL

Microlens parallax measurements resolve the principal degeneracy of the lens geometry by locating the lens along the line of sight, thereby reducing by an order of magnitude uncertainty in the masses of the lens stars and their planets.

Most microlensing events are described by three parameters ( $t_0, u_0, t_E$ ), their time of maximum, impact parameter (in units of Einstein radius  $\theta_E$ ) and Einstein timescale:

$$t_E = \frac{\theta_E}{\mu}; \quad \theta_E^2 = \kappa M \pi_{\text{rel}}; \quad \kappa = \frac{4G}{c^2 \text{AU}} = 8.1 \frac{\text{mas}}{M_\odot}. \quad (1)$$

Here  $\pi_{\text{rel}}$  and  $\mu$  are the lens-source relative parallax and proper motion, respectively, and  $M$  is the lens mass. Thus,  $M$ ,  $\pi_{\text{rel}}$  and  $\mu$  are generally not known separately, but only through the peculiar combination of them in the observable  $t_E$ .

In the case of planetary microlensing events, however, one very often measures  $\theta_E$ . This is because the planets give rise to sharp “caustic” features in the lightcurve, which is smoothed out by an observable “smearing length”  $t_*$  according to the angular source radius  $\theta_*$ . Since  $\theta_*$  can be measured using standard techniques,

(Yoo et al., 2004), one can determine the proper motion  $\mu = \theta_*/t_*$ , and so  $\theta_E = \mu t_E$ . This, by itself, reduces the 3-fold degeneracy by one dimension to 2-fold. It is this degeneracy that can be resolved by measuring the microlens parallax  $\pi_E$ ,

$$\pi_E = \pi_{\text{rel}} \frac{\mu}{\mu}; \quad \pi_E = \frac{\pi_{\text{rel}}}{\theta_E} \quad (2)$$

Before stating why  $\pi_E$  has this form or how it is measured, it is important to emphasize that (together with  $\theta_E$ ) this measurement retrieves the lens mass and relative parallax,

$$M = \frac{\theta_E}{\kappa \pi_E}; \quad \pi_{\text{rel}} = \theta_E \pi_E. \quad (3)$$

Then, since the source parallax  $\pi_s$  is usually quite well known, the lens distance can be determined  $D_l = \text{AU}/(\pi_{\text{rel}} + \pi_s)$ .

## 3. HOW MICROLENS PARALLAXES ARE MEASURED

If the observer changes position by a vector distance  $\Delta \mathbf{x}$ , then the apparent separation of the lens and source will change by  $\Delta \theta = (\pi_{\text{rel}}/\text{AU}) \Delta \mathbf{x}$ . Hence, the separation in the Einstein ring will change by

$$\Delta \mathbf{u} = \frac{\Delta \theta}{\theta_E} = \frac{\pi_{\text{rel}}}{\theta_E} \frac{\Delta \mathbf{x}}{\text{AU}} = \pi_E \frac{\Delta \mathbf{x}}{\text{AU}} \quad (4)$$

Because a displacement  $\Delta \mathbf{u}$  in the Einstein ring leads to measurable changes in magnification, and since  $\Delta \mathbf{x}$  is of course known, such displaced observations can yield a parallax measurement.

The overwhelming majority of microlens parallax measurements to date have used the moving platform of Earth. Unfortunately, most microlensing events are short  $t_E \lesssim 30$  days, and Earth does not deviate very far from rectilinear motion during such times. Hence, out of roughly 10,000 microlensing events discovered to date, less than 100 have parallax measurements.

By contrast, observatories in solar orbit are well matched to microlens parallax requirements. For typical bulge lenses ( $M \sim 0.5 M_\odot$ ,  $\pi_{\text{rel}} \sim 10 \mu\text{as}$ ), the projected Einstein radius is  $\tilde{r}_E \equiv \text{AU}/\pi_E \sim 20 \text{AU}$ , while for typical disk lenses ( $M \sim 0.5 M_\odot$ ,  $\pi_{\text{rel}} \sim 100 \mu\text{as}$ ),

$\tilde{r}_E \sim 6 \text{ AU}$ . Thus, at  $\Delta x \sim 1 \text{ AU}$ , such a satellite is far enough away to cause a significant change in the magnification, but not so far away as to be outside the Einstein ring (so no magnification).

#### 4. K2 FIELD 9 OBSERVING PLAN

There are six major constraints on K2 parallax microlensing observations. First, it must be directed toward the Galactic bulge microlensing fields, which (due to high density of lenses and source and large angular size) has orders of magnitude more microlensing events than any other region of the sky. These will have round-the-clock 10-min-cadence ground-based observations from a total of 5 wide-field microlensing telescopes (weather permitting). Second, the K2 bore-sight is constrained to an essentially 1-D track that is slightly displaced from the K2 orbital plane, which itself is very near the ecliptic. This, by itself constrains K2 to two observing windows, one (centered in May) in the velocity direction and the other (centered in November) in the anti-velocity direction. Third, observations must take place simultaneously with Earth observations. This eliminates the November window. Fourth, the window is restricted to an 83-day interval that is precisely determined by the pointing direction. Fifth, targets cannot be uploaded in real time, so a pre-defined contiguous set of pixels must be observed, rather than adding new microlens targets as they are discovered. Sixth, recorder and communications restrictions (as well as pixels reserved for other programs) restrict this field to  $5.34 \text{ deg}^2$ .

Figure 1 illustrates a near-optimal choice of pointing, given these constraints. With the bore-sight at (18:01:25.08, -21:46:47.3), the observation window is 7 Apr – 29 Jun. Approximately 38% of all microlensing events peak in this 83 day window. Further optimization is possible, partly by choosing a more complicated polygon to avoid obvious “dead areas”. But also, some of these areas are not actually dead but just infrequently observed for technical reasons that could be set aside for the duration of the K2 microlensing campaign. Hence, it is plausible that a further 10% improvement is possible.

#### 5. K2 FREE-FLOATING PLANETS

Microlensing is the *only* method to detect old free-floating planets (FFPs) because all other techniques rely on light from either the host or the planet. Sumi et al. (2011) have detected a strong excess of short ( $t_E \sim 1 \text{ day}$ ) events that they attribute to FFPs. If this hypothesis is correct, then there are roughly 2 FFPs for each star, with characteristic mass similar to Jupiter. Actually, because of the degeneracies embedded in Equation (1), these short timescales could in principle be due to high  $\mu$  or low  $\pi_{\text{rel}}$ , rather than simply low  $M$ . Now, in fact, high  $\mu$  is in most cases ruled out because the objects would be moving so fast that they would not be confined to the Galaxy. However, low  $\pi_{\text{rel}}$  is a serious possibility for any particular short event. The only way to definitively confirm individual lenses as FFPs, and so to start measuring their properties is

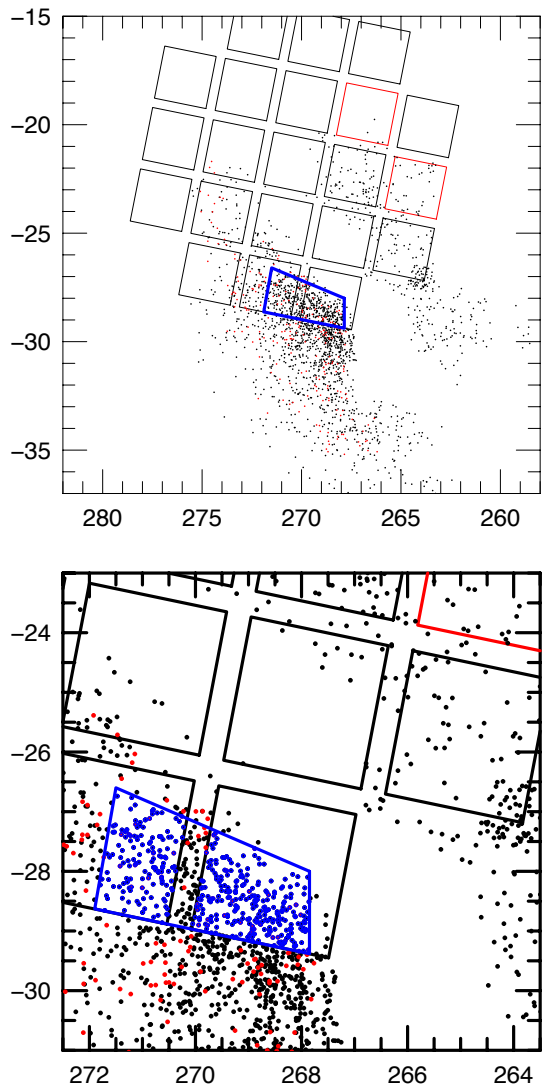


**Figure 1.** Near optimal choice of K2 microlensing field. Black (red) squares are active (dead) chips (subdivisions not shown). Black (red) points are OGLE (MOA-only) 2013 microlensing events. Blue quadrilateral is simple first cut at  $5.34 \text{ deg}^2$  microlensing zone. In lower panel, blue points are the 420 events from 2013 that lie in this zone out of 2200 total. Further optimization is possible (see text).

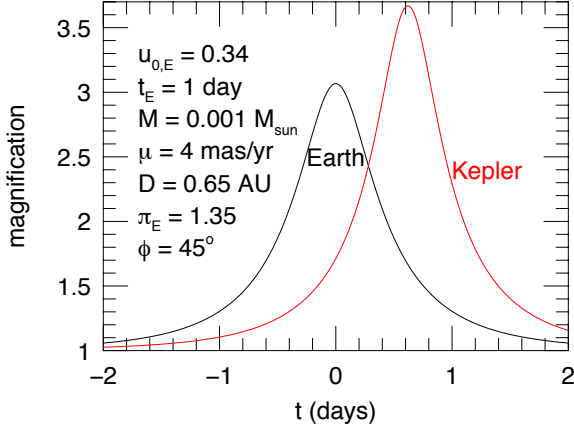


**Figure 2.** Illustration of **confirmation** of microlensing free-floating planet (FFP) candidate by K2. Earth observations (black) show a short ( $t_E = 1$  day) event. K2 data (red) show peak that is both substantially displaced in time and has different impact parameter (so different height), implying that the microlens parallax ( $\pi_E = (\pi_{\text{rel}}/\kappa M)^{1/2}$ ) is large. This demonstrates that the short timescale is in fact due to low lens mass  $M$ , i.e., planet.

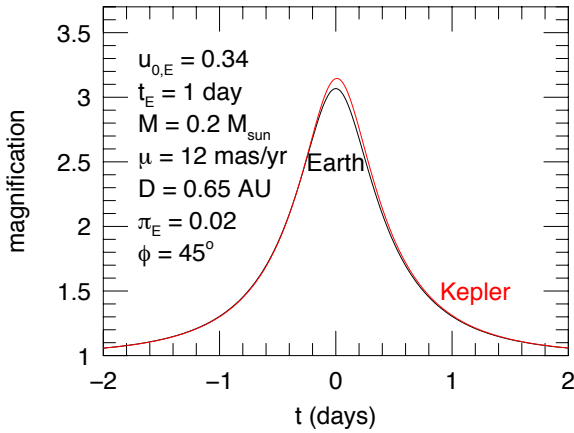


**Figure 3.** Illustration of **contradiction** of microlensing free-floating planet (FFP) candidate by K2. Earth observations (black) show a short ( $t_E = 1$  day) event. K2 data (red) show very similar lightcurve to that seen from Earth, implying that the microlens parallax ( $\pi_E = (\pi_{\text{rel}}/\kappa M)^{1/2}$ ) is small. This demonstrates that the short timescale is in fact due to low lens lens-source relative parallax  $\pi_{\text{rel}}$ , rather than a low-mass (i.e., planetary) lens.

to obtain microlens parallaxes. And K2 is the *only* foreseeable way to measure these parallaxes. Figures 2 and 3 illustrate how this works. The key point is that because K2 is observing a large field (and not a designated set of events), it can “catch” short events even before they are recognized from Earth.

To estimate the expected number of FFPs, we start with the 2200 stellar events per year. The event rate is 20 times lower (because the Einstein radii are 20 times smaller). There are two planets for each star. Only 38% of events peak in the K2 time window, and only 420/2200 occur in the K2 sky window. Hence, we expect

$$N_{\text{ffp}} = 2200 \times (1/20) \times 2 \times 38\% \times (420/2200) = 16. \quad (5)$$

The parallax measurements will not only confirm the planetary nature of these events but give the first measurement of their mass function. This is because

$$M = \frac{\mu t_E}{\kappa \pi_E}. \quad (6)$$

All quantities on the rhs are measured except  $\mu$ , and  $\mu$  is typically drawn from a narrow distribution  $3 \text{ mas yr}^{-1} \lesssim \mu \lesssim 7 \text{ mas yr}^{-1}$ .

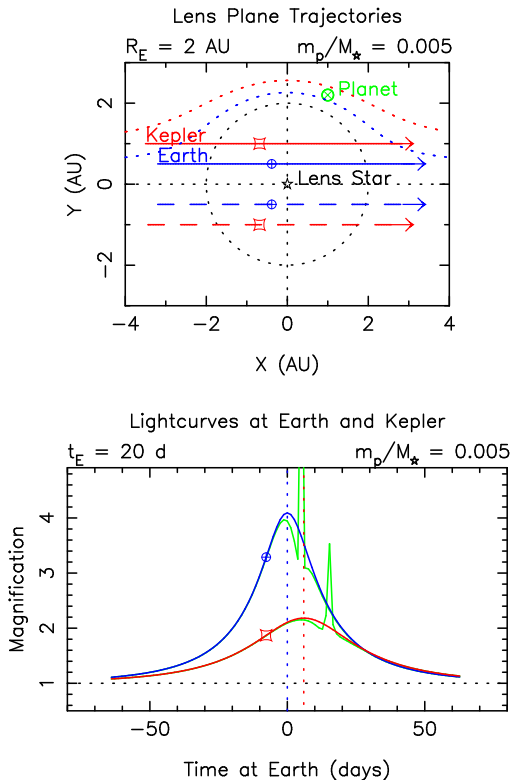
## 6. K2 PLANET MASS MEASUREMENTS

Figure 4 (from Gould & Horne 2013) illustrates how K2 will measure microlens planet masses. What makes it possible to turn parallax measurements into mass measurements is the planetary anomaly, which permits measurement of  $t_*$  (and so  $\theta_E = \theta_* t_E / t_*$ , and so  $M = \theta_E / \kappa \pi_E$ ). See Section 2. These “finite-source effects” are usually measured but not always. However, with continuous K2 data and higher cadence ground data from the new KMTNet survey, the probability that they will be measured from K2 and/or Earth is very high. Currently there are 15 OGLE+MOA planets discovered per year. We expect that this number will approximately double with the onset of KMTNet, and we further augment this number by 1.5 to account for the fact that (due to parallax) K2 will often detect the planetary anomaly when it is missed from Earth. This leads to an estimate of planetary mass measurements

$$N_{\text{planet-mass}} = 15 \times 38\% \times (420/2200) \times 3 = 3.3 \quad (7)$$

## 7. DATA ANALYSIS

We are developing a data analysis pipeline (spearheaded by Matthew Penny at OSU) to cope with the crowded fields that will be observed in the K2 microlensing campaign. The pipeline will be adapted from an existing Difference Imaging Analysis (DIA) pipeline that is currently employed extremely successfully by the KELT survey, which experiences similar crowding conditions to Kepler (when measured as stars per pixel) and a similarly stable PSF (because KELT’s arcminute PSF is far larger than any seeing variations). The pipeline will be refined using a combination of real K2 data from crowded open and globular clusters in the previous K2 fields (e.g., particularly NGC 2158 in Campaign



**Figure 4.** Illustration of four-fold degeneracy derived from comparison of *Kepler* and ground based lightcurves. Upper panel shows two possible trajectories of the source relative to the lens for each of *Kepler* (red) and Earth (blue) observatories. Each set would give rise to the same point-lens lightcurve in the lower panel (same colors), leading to an ambiguity in the Earth-*Kepler* separation (distance between red circle and blue square) relative to the Einstein ring. In this particular case, the planet causes deviations to both lightcurves (green), thus proving that the trajectories are on the same side of the Einstein ring. More generally, the planet would appear in only one curve, leaving the ambiguity open. In this case, it would be resolved by more subtle differences in the Einstein timescale due to small Earth-*Kepler* relative motion (which is not captured in this idealized diagram). See Gould & Horne (2013) for details.

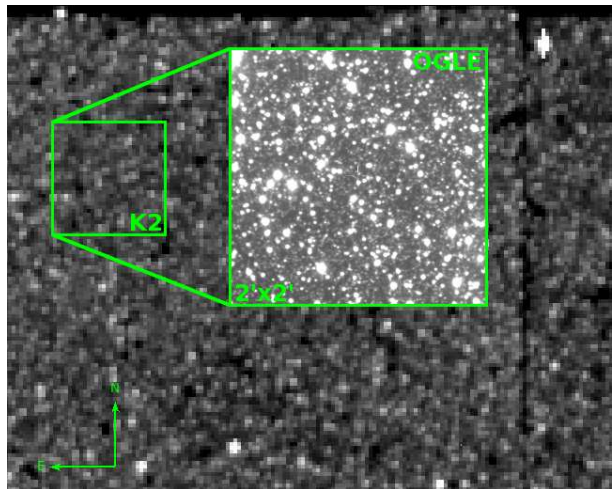


**Figure 5.** Simulated K2 image of a microlensing survey field built using OGLE photometric catalogues and the Kepler pixel response function. Zoom in shows a typical OGLE reference field. It is likely that DIA reference frames for K2 will be built from much higher-resolution ground based images, e.g. from OGLE V and I images or DECam Bulge Survey g and r images.

0, whose core closely resembles a bulge star field) and realistic simulated images built from deep OGLE star catalogs and the Kepler pixel response function (PRF, Bryson et al. 2010a). Later, we may use the more sophisticated Kepler end-to-end model for image simulations (Bryson et al., 2010b).

## 8. CONCLUSION

K2 can confirm (or contradict) about 16 FFP candidates. If confirmed, then each candidate will yield a mass estimate with factor 1.5 precision. This will enable the first measurement of the FFP mass function.

K2 will measure individual masses for about 3 bound planets. 1/3 (i.e., about 1) of these will be new discoveries (i.e., no ground-based detection), while the remaining 2/3 will be detected from the ground, but would not have mass measurements without K2.

K2 will also make mass measurements of brown-dwarf binaries as well as other binary stars, and will yield parallaxes for more than 100 microlensing events that are generated by single stars. This will enable other science that is interesting but not at the same level of priority.

K2 data analysis presents special challenges. Our team is already working on a pipeline to meet those challenges.

## REFERENCES

- Bryson S.T. et al. 2010a, ApJ, 713, L97
- Bryson S.T. et al. 2010b, SPIE, 7738
- Gould, A. & Horne, K. 2013, ApJ779, L28
- Refsdal, S. 1966, MNRAS, 134, 315
- Sumi, T. et al. 2011, Natur, 473, 349
- Yoo, J. et al. 2004, ApJ, 603, 139